EFFECT OF COOLING RATE DURING HEAT TREATMENT ON MARTENSITIC-BAINITIC CLASS ALLOY STEEL MICROSTRUCTURE AND PROPERTIES

M. V. Maisuradze,[1] **A. A. Kuklina,**[2] **M. A. Ryzhkov,**[3]
D. I. Lebedev,[4] **and E. V. Antakov**[5]

UDC 669.158.8

The microstructure and mechanical properties of engineering steels with high supercooled austenite stability after cooling at different rates from the austenitizing temperature are studied. Thermokinetic diagrams are plotted for supercooled austenite transformation and temperature-time intervals are determined for structural component formation during continuous cooling. In order to evaluate mechanical properties trajectories and cooling rates are established by experiment for specimens in various media, i.e., oil, still air, and a special container filled with cast iron shavings. It is shown that when the experimental cooling path is superimposed on a thermokinetic curve it is necessary to consider instantaneous cooling rates in different temperature ranges. The effect of cooling intensity on mechanical properties of steels of different composition is established quantitatively. It is found that the impact strength of steels of different alloy systems depends in different ways on cooling rate.

Keywords: steel, heat treatment, cooling rate, bainite, martensite, mechanical properties, thermokinetic diagram.

Introduction

In practice it is very difficult to prepare an entirely martensitic structure during steel object quenching in the standard quenching media used. Moreover, this is not always expedient since rapid cooling during quenching may lead to formation of an increased level of residual stresses, component deformation, and even cracking [1–3]. In view of this within industry there is extensive use of alloy steels of bainitic and martensitic classes having a slow rate for suppression of supercooled austenite diffusion transformations [4–8]. During quenching components of similar steels with application of slow cooling (in air, within heat-insulated blocks, etc.) there is formation within them of a bainitic-martensitic microstructure without separation of ferrite or pearlite.

However, it is well known that bainite formed in different temperature ranges may have significantly different properties [9–11]. Upper bainite formed at above 400°C in the majority of low and medium carbon steels normally has low impact strength, toughness, and strength, and lower bainite formed in the temperature range below 300°C, including within the martensitic transformation region, may provide a combination of steel high strength, ductility, and toughness [12, 13].

[1] B. N. Yeltsin Ural Federal University, Ekaterinburg, Russia; e-mail: spirallog@gmail.com.

[2] B. N. Yeltsin Ural Federal University, Ekaterinburg, Russia; Ural State Mining University, Ekaterinburg, Russia; e-mail: kuklina.aleksandra@rambler.ru.

[3] B. N. Yeltsin Ural Federal University, Ekaterinburg, Russia; e-mail: mt-243@mail.ru.

[4] B. N. Yeltsin Ural Federal University, Ekaterinburg, Russia; M. N. Mikheev Institute of Metal Physics, Ural Section, Russian Academy of Sciences, Ekaterinburg, Russia; e-mail: dumohleb@mail.ru.

[5] B. N. Yeltsin Ural Federal University, Ekaterinburg, Russia; e-mail: antakov14@yandex.ru.

Table 1
Test Steel Chemical Composition, wt.%

Steel	C	Cr	Mn	Si	Ni	Mo	V	S	P	Cu
18Kh2N4MA	0.19	1.44	0.40	0.34	4.05	0.31	0.01	0.005	0.007	0.10
20Kh2G2SNMA	0.22	1.96	2.02	0.96	1.09	0.31	0.01	0.002	0.010	0.09
25KhN3MA	0.26	1.18	0.66	0.26	2.74	0.19	0.01	0.019	0.010	0.12
25Kh2N4MA	0.27	1.42	0.43	0.26	4.14	0.29	0.01	0.011	0.011	0.16
25Kh2GSMA	0.28	1.61	1.09	0.87	0.24	0.15	0.02	0.011	0.020	0.22
30Kh3MF	0.30	2.23	0.65	0.24	0.21	0.21	0.11	0.030	0.009	0.18

During steel component heat treatment implementing continuous cooling from the austenitizing to room temperature, depending on cooling rate and supercooled austenite stability (which is determined by steel chemical composition), it is possible to form a complex microstructure combining upper and lower bainite, martensite and also some amount of untransformed residual austenite [14–16]. It is almost impossible to predict the mechanical properties of these structures since they will be determined by the combined effect of many factors: the structural component ratio, chemical composition, fine structure morphology, amount and degree of residual austenite, presence of carbide phase precipitates within bainite, etc.

The aim of the work is analysis of the effect of cooling rate during heat treatment on formation of a set of properties and microstructure of a number of structural steels of bainitic and martensitic classes used in domestic and overseas industry.

Research Materials and Procedure

The microstructure and mechanical properties are studied for industrial structural steels of bainitic and martensitic classes whose chemical composition is provided in Table 1. In the original condition test steels have a globular cementite structure within a ferrite matrix. The microstructure of globular cementite with a ferrite matrix forms as a result of normalizing and subsequent high-temperature tempering. Steel hardness in the as-supplied condition was not more than 289 *HB*.

Test steel specimen (section 15×15 mm, length 65 mm) laboratory heat treatment was conducted in a SNOL type laboratory chamber furnace. The heating temperature was A_{c3} + (30–50°C), and the exposure time at the austenitizing temperature was 60 min. Cooling was conducted in quenching oil I20A at 40–60°C, and also within still air at 20–25°C. In order to implement slow specimen cooling before placement within a furnace it was packed into a container of heat-resistant steel within a layer of fine cast iron turnings and then covered with shavings from above. The exposure time for a container with a specimen in a furnace at the austenitizing temperature was 120 min in order to provide charge heating. The cooling rate for a specimen in a container was in still air. After cooling specimens were subjected to low-temperature tempering at1 80–200°C for 3 h in order to remove internal stresses.

Evaluation of the cooling rate achieved in an experiment was conducted by means of a special thermal probe made of austenitic steel whose structure and operating principle have been described in detail in [17–19].

Experimental cooling trajectories were obtained by means of a thermal probe realized during specimen cooling in oil, in air, and with use of a container with cast iron shavings.

Structural transformations in the test steels with continuous cooling were studied in a LINSEIS L78 R.I.T.A dilatometer. Specimen (diameter 4 mm, length 10 mm) heating temperature was A_{c3} + (30–50°C). The exposure time at the austenitizing temperature was 15 min. Dilatometric specimens were cooled at a constant rate in the range 0.1–30°C/sec. In the course of an experiment the change in specimen relative elongation was recorded in relation to temperature. Temperature-time ranges for supercooled austenite transformation were evaluated according breaks in the dilatograms obtained. For the beginning or end of transformation points were adopted at which a marked deviation for curves from a straight line was obtained describing the linear section for a dilatograms before and after realizing transformation. Information obtained in this way about the temperature and time transformation ranges with different cooling rates made it possible to construct thermokinetic diagrams (TKD) for supercooled austenite decomposition within the test steels [14].

Uniaxial tensile testing according to GOST 1407 was performed at room temperature on cylindrical specimens with a gauge length diameter of 6 mm and an initial gauge length of 30 mm using an Instron test machine. Impact bending tests were conducted at room temperature according to GOST 9454 in an MK-30 pendulum hammer with maximum failure energy of 300 J. Specimens 55 mm long with a V-shaped stress concentrator were used. The specimens cross section in the area of a stress concentrator was 8×10 mm. No fewer than six specimens were tested for each steel with each heat treatment regime; the error for results obtained was determined by a standard statistical method and was not more than 3%.

Microhardness tests were conducted by the Vickers method according to GOST 9450 using an HSV-1000A microhardness meter with a load of 300–1000 g. Macrohardness testing was carried out by the Rockwell method according to scale C (GOST 9013).

In order to reveal steel specimen microstructure there was grinding, polishing, and etching in 4% ethanolic nitric acid solution. The microstructure was analyzed by means of a MEIJI IM7200 optical microscope at 50–1000-fold magnification.

Experimental Results and Discussion

By means of a special thermal probe [17–19] temperature trajectories were established by experiment obtained with implementing cooling from 850 ± 10°C in oil, in still air, and with use of a container filler filled with cast iron shavings (Fig. 1a). The thermal probe cooling rate was determined (Fig. 1b) that for the bainitic and martensitic transformation temperature ranges in low-carbon and medium-carbon steels (50–200°C) was on average: 25°C/sec with oil cooling; 1.0°C/sec with cooling in still; 0.2°C/sec with cooling in a container. Therefore experimental conditions were implemented for cooling rates differing by more than a factor of 100.

Dilatometric study made it possible to evaluate the temperature-time ranges for supercooled austenite transformation and also the microstructure formed within steels with different constant cooling rates (Fig. 2). In particular it was established that in steels 25KhN3MA, 25Kh2GSMA, and 30Kh3MF with cooling at a rate of 0.3°C/sec there is formation of a significant amount of upper bainite, and a "feathered" and "globular" typical for the majority of structural steels (Fig. 3a–c). In addition, in steels 25Kh2GSMA and 30Kh3MF with cooling at a rate of 0.1–0.3°C/sec there is formation of supercooled austenite transformation diffusion products (see Fig. 3b, c). In steel 18Kh2N4MA a significant amount of bainite only forms with a cooling rate of 0.1°C/sec, but with an increase in cooling intensity to 0.3°C/sec the amount of bainite within the structure is not more than 20% (Fig. 3d). Steels 25Kh2N4MA and 20Kh2G2SNMA have supercooled austenite stability, and even with slow cooling at a rate of 0.1–0.3°C/sec there is predominantly formation within them of a low-temperature structural component of package morphology (Fig. 3e, f). With a cooling rate of 1–3°C/sec, corresponding to cooling
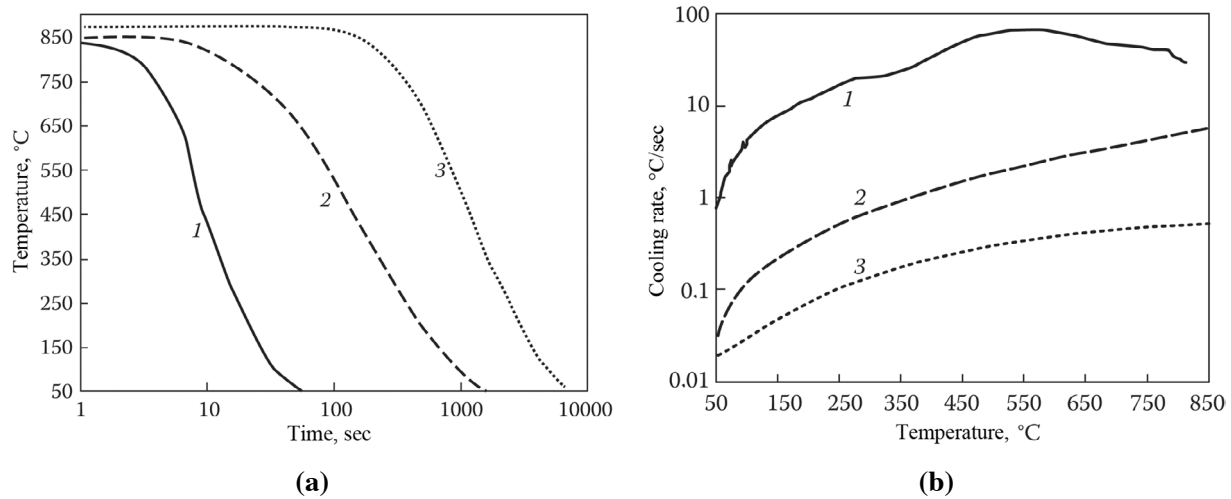
Fig. 1. Thermal probe cooling trajectories obtained under experimental conditions (a) and dependence of thermal probe cooling rate on temperature (b): *1*) oil cooling; *2*) air cooling; *3*) cooling in container.

in still air, within the test steel structure there is formation of a mixture of bainite and martensite having predominantly package morphology (with the exception of steel 30Kh3MF, for which there is typically formation of a significant amount of upper bainite in a wide cooling rate range 0.1–3°C/sec).

Dilatometric study of supercooled austenite transformation in test steels showed that within the experimental cooling rate range, achieved under laboratory conditions (Fig. 1), within the structure there will be formation of bainite and martensite in different ratios (Fig. 2). Slow cooling within a container with cast iron shavings should not lead to formation of ferrite and pearlite mixture within steels 25Kh2GSMA and 30Kh3MF since with use of a container within the transformation temperature range (750–600°C) the cooling rate is 0.4–0.5°C/sec. Oil cooling provides an entirely martensitic for all test steels.

It has been established that the strength of all test steels decreases with an increases in cooling intensity (Fig. 4), which is mainly connected with an increase the proportion of bainite within a structure. However, for steels 20Kh2G2SNMA and 25Kh2N4MA strength changes to a lesser extent. This effect is connected with the greater stability of supercooled austenite for these steels compared with the rest. Within the structure of steel 25Kh2N4MA after cooling in air and in oil a predominantly martensitic structure is observed (Fig. 5a, b), and with cooling in a container there is separation of a considerable amount of bainite (Fig. 5c), which leads to a reduction in strength. For steel 20Kh2G2SNMA after cooling in air, in oil, and in a container the morphology of the microstructure formed does not change markedly (Fig. 6). Nonetheless, an increase in the strength reduction observed is probably connected with formation simultaneously with martensite of a small amount of lower bainite having complex morphology and also processes of self tempering of the structural component formed.

In all of the test steels the least strength with the cooling rates in question applies to steel 18Kh2N4MA that is connected with a low carbon content within it. Due to this the steel provides maximum impact strength, from 1.05 MJ/m^2 with oil cooling to 1.45 MJ/m^2 with slow cooling in a container (Fig. 7). A similar increase in impact strength with a reduction in cooling rate is probably typical for steels with a nickel content of more than 4 wt.%. In this case the impact strength of steel 25Kh2N4MA is almost unchanged, although a tendency is retained for an increase with a reduction in cooling rate, although not as clearly as for a steel 18Kh2N4MA. For steel 20Kh2G2SNMA there is atypical uniform reduction in impact strength, and fro steels 25KhN3MA, 25Kh2GSMA, and 30Kh3MF a marked reduction in impact strength is observed only with a reduction in cooling rate from 1 to 0.2°C/sec (in this case as a result of air cooling at a rate of 1°C/sec the level of impact strength for steels 25KhN3MA and 25Kh2GSMA is higher by 10–15% than after oil quenching).
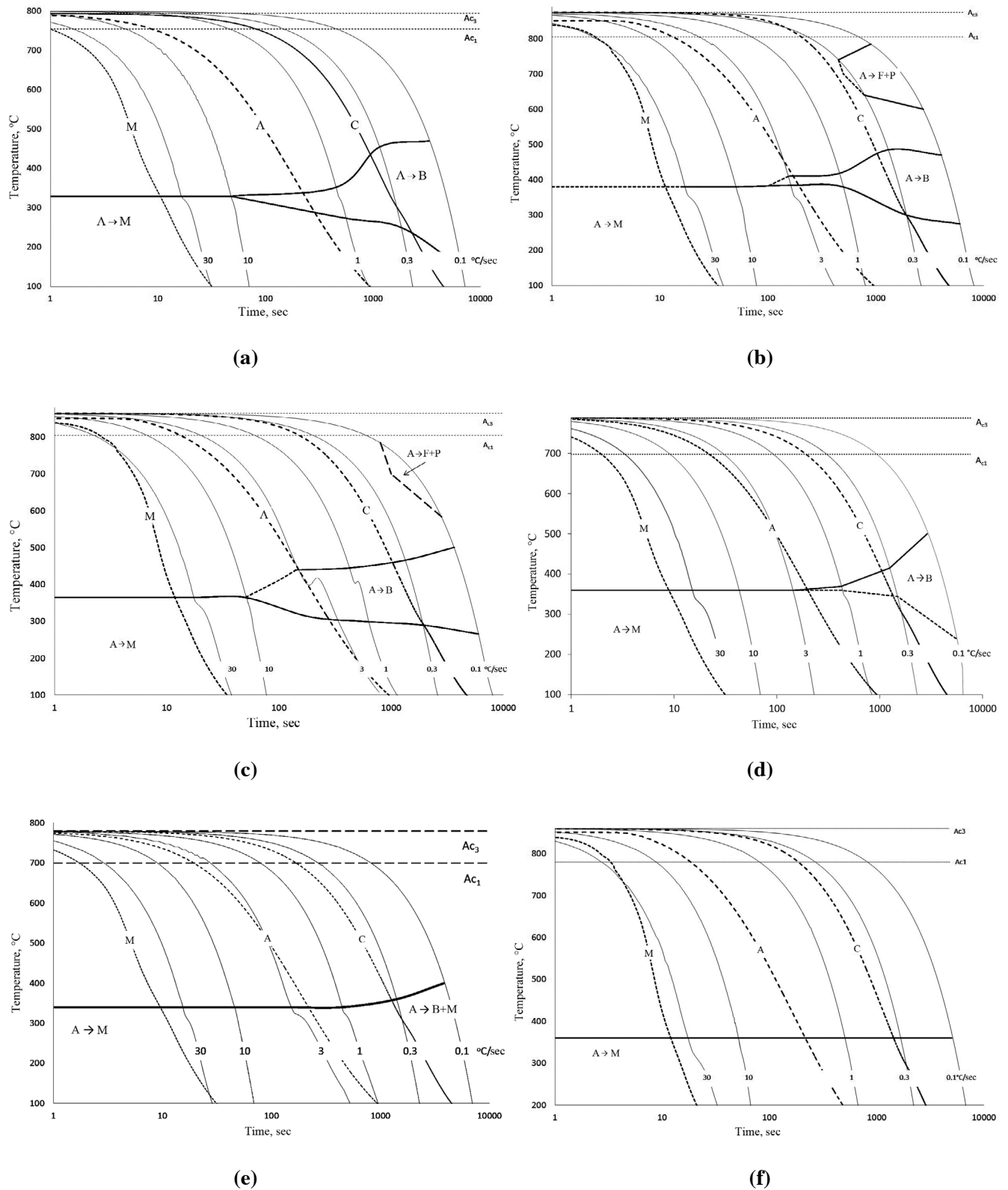
Fig. 2. Supercooled austenite thermokinetic transformation diagram within test steels with superimposed experimental cooling trajectories (M is oil; A is air; C is container): (a) 25KhN3MA; (b) 25Kh2GSMA; (c) 30Kh3MF; (d) 18Kh2N4MA; (e) 25Kh2N4MA; (f) 20Kh2G2SNMA.
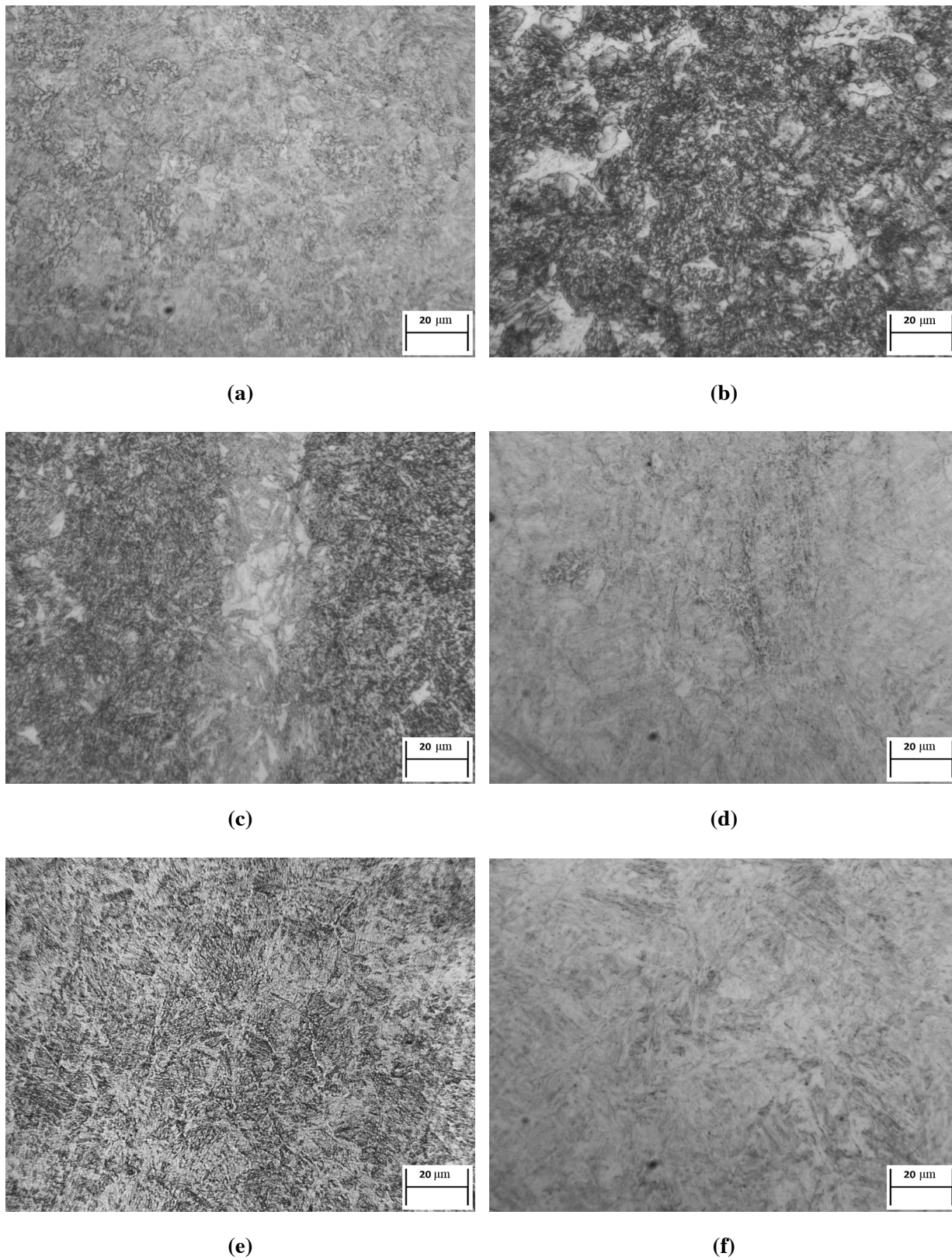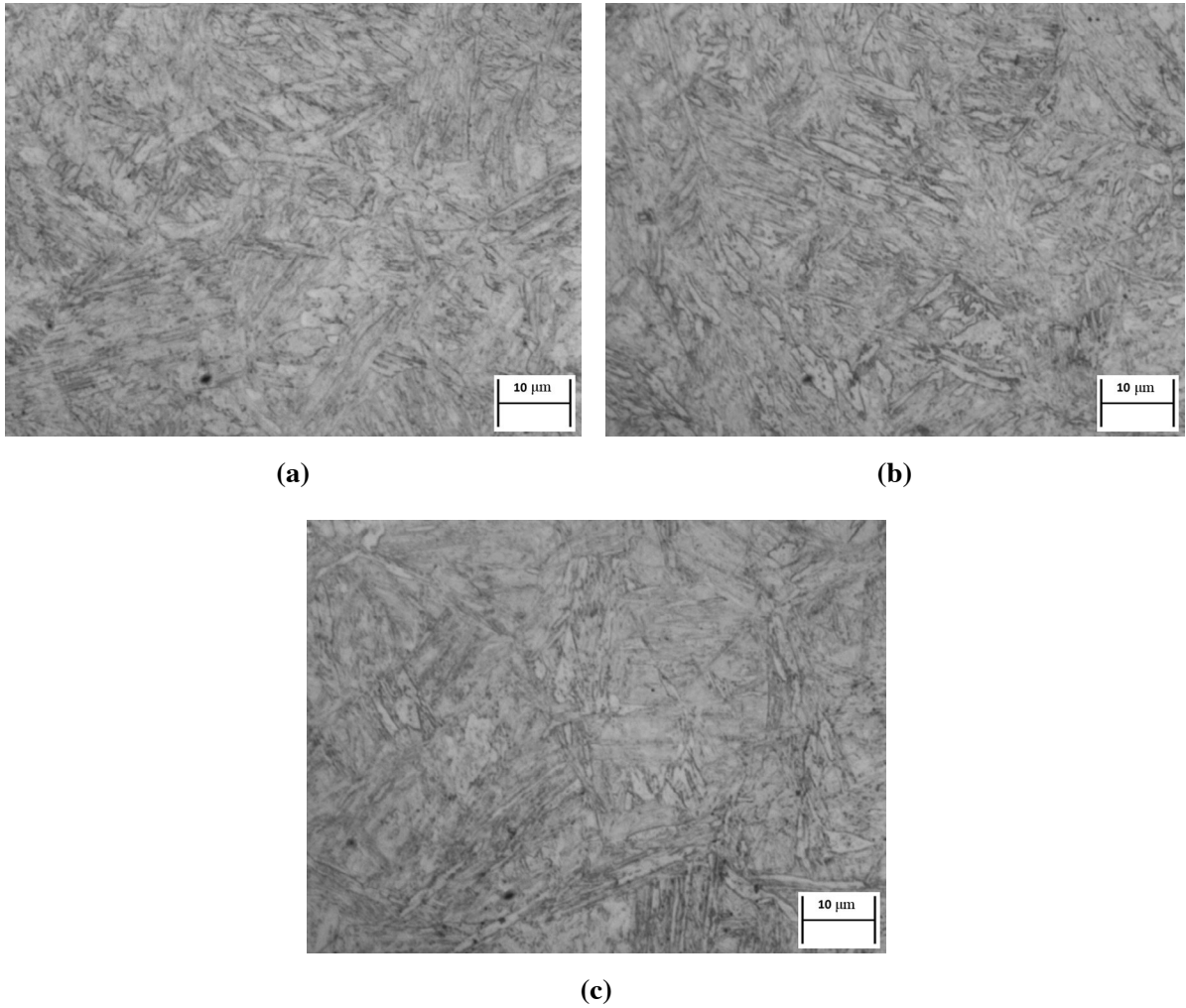
Fig. 3. Test steel microstructure after cooling at a rate of 0.3°C/sec: (a) 25KhN3MA; (b) 25Kh2GSMA; (c) 30Kh3MF; (d) 18Kh2N4MA; (e) 25Kh2N4MA; (f) 20Kh2G2SNMA (arrows show upper bainite region).
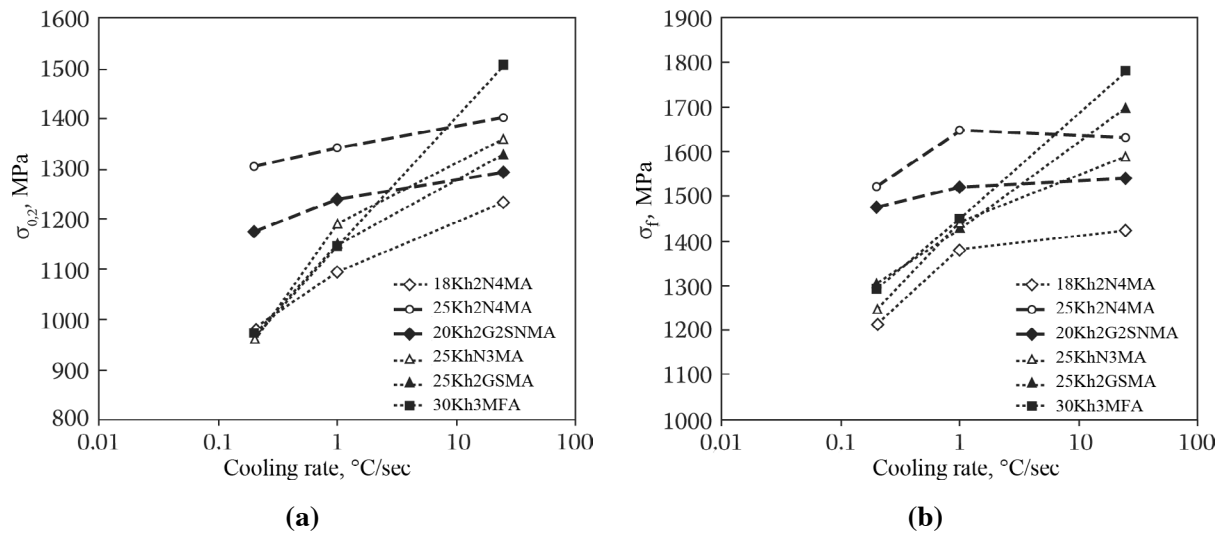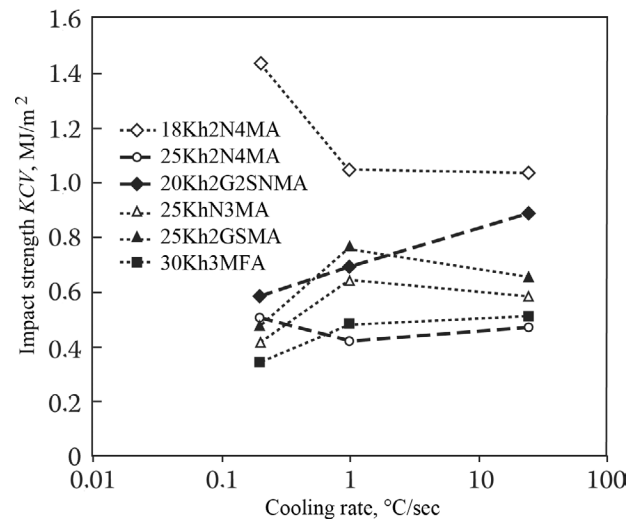
Fig. 4. Test steel strength properties in relation to cooling intensity: (a) yield strength; (b) ultimate strength.
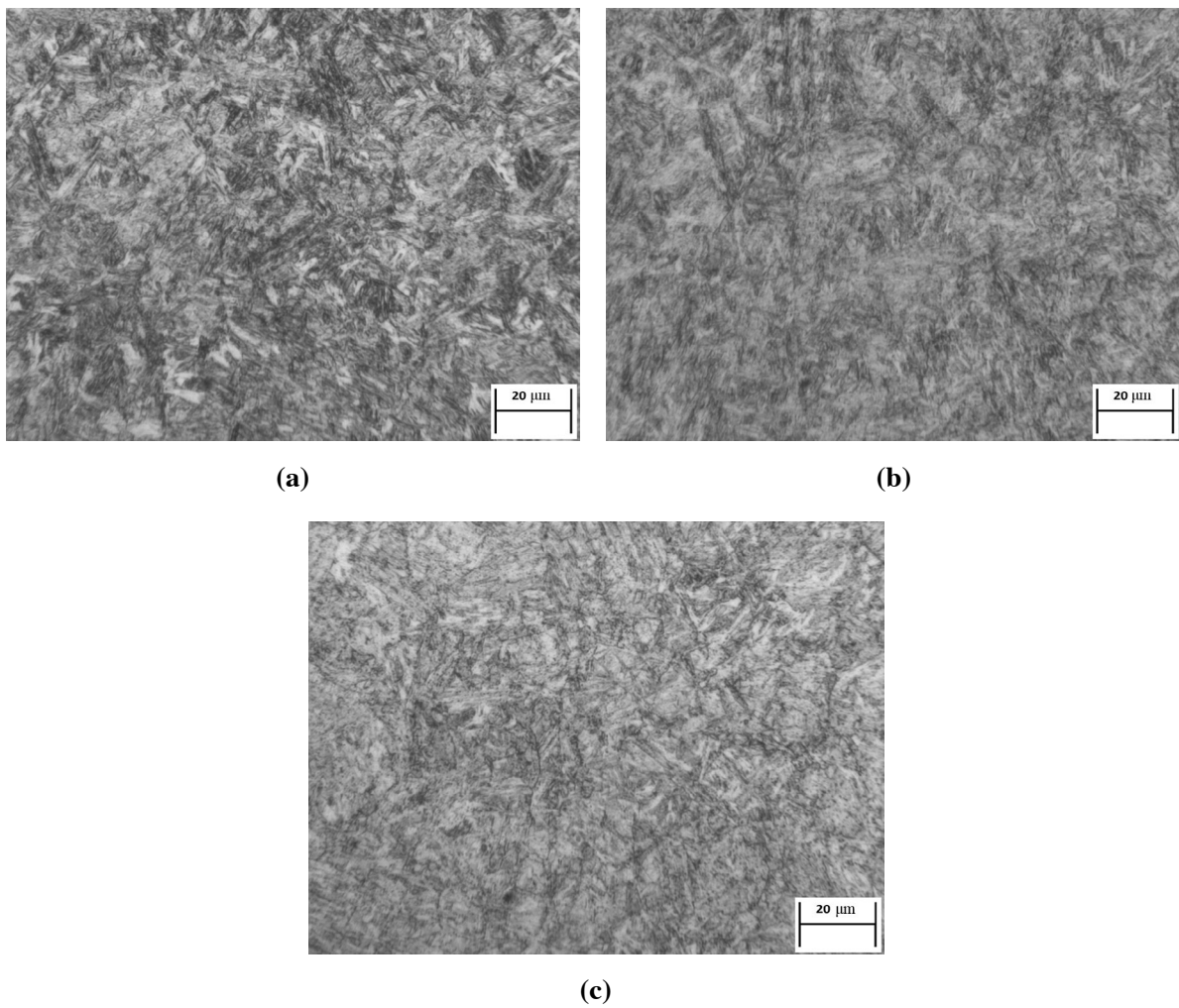
Fig. 5. Steel 25Kh2N4MA microstructure after cooling with different intensity: (a) oil; (b) still air; (c) container.
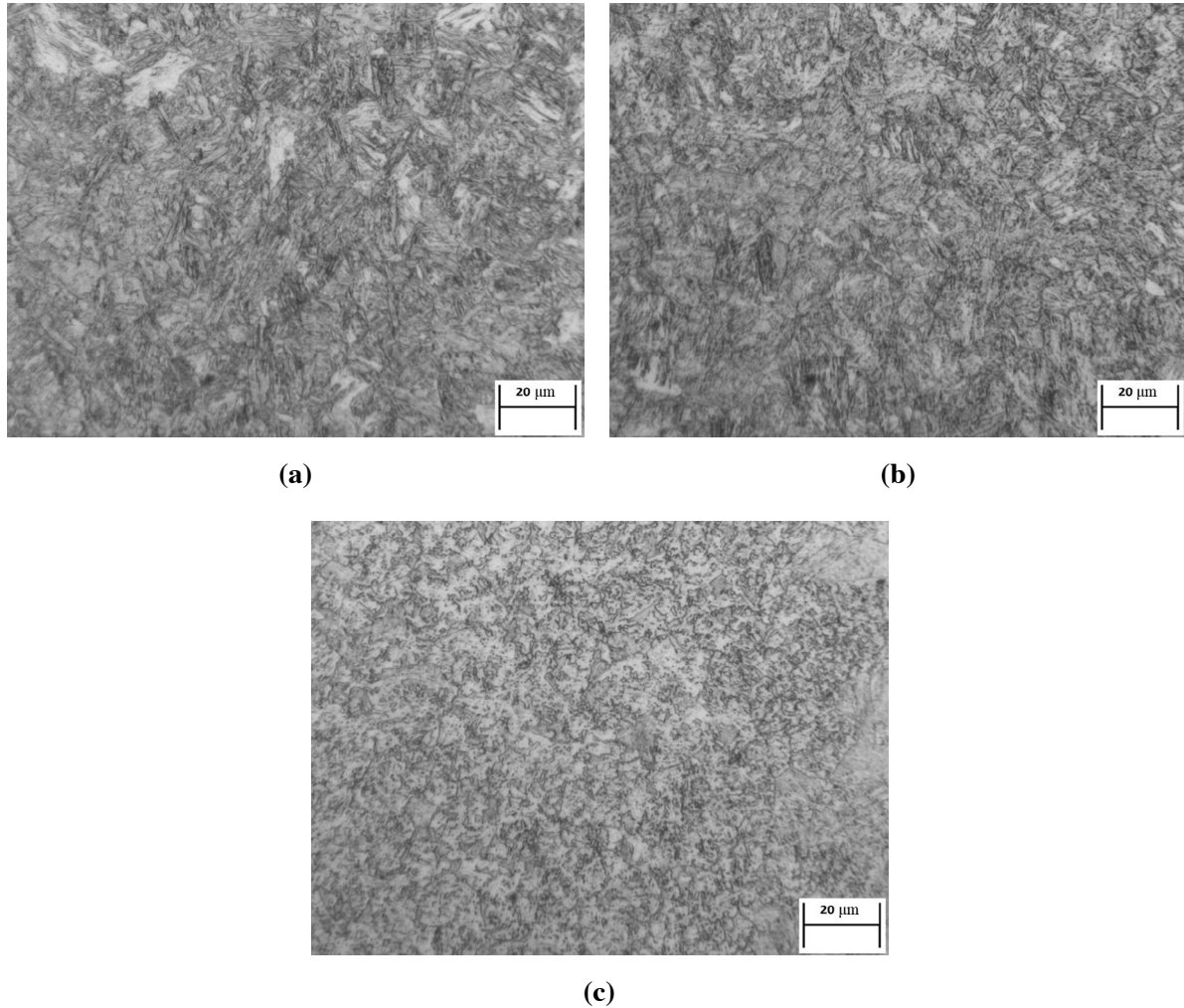
(a)

(b)

(c)

Fig. 6. Steel 20Kh2G2SNMA microstructure after cooling with different intensity: (a) oil; (b) still air; (c) container.

**Fig. 7.** Dependence of test steel impact strength on cooling intensity.

(a)

(b)

(c)

Fig. 8. Steel 18Kh2N4MA microstructure after cooling with different intensity: (a) oil; (b) still air; (c) container.

The microstructure of steel 18Kh2N4MA after oil cooling is martensite (Fig. 8a), after air cooling some amount of bainite is observed with martensite (Fig. 8b), and after cooling in a container with cast iron shavings the microstructure predominantly consists of bainite (Fig. 8c). The microstructure morphology in this case corresponds to upper bainite (granular "loose" structure, absence of clearly defined packages) that theoretically should have reduced impact strength. Nonetheless, formation during the slow cooling process of upper bainite for steel 18Kh2N4MA is distinguished by very high impact strength (1.45 mJ/m^2), and therefore probably facilitated by a significant nickel content that increase increases steel α-phase ductility as a whole [20], and a reduced carbon content as a result of which the amount of carbide particles separated during bainitic transformation appears to be lower than in the case of other test steels studied. Cooling of steel 18Kh2N4MA specimens in the bainite formation range proceeds with an average rate of $0.2°$C/sec that provides an almost completely uniform bainitic microstructure.

It should be noted that application of experimental thermal trajectories obtained during cooling of specimens using variable cooling rates to steel TKD plotted with constant cooling rates is not entirely correct. This is seen clearly on the example of steel 18Kh2N4MA in the case of implementing cooling within a container with cast iron shavings the experimental cooling trajectory intersects the region of bainitic transformation
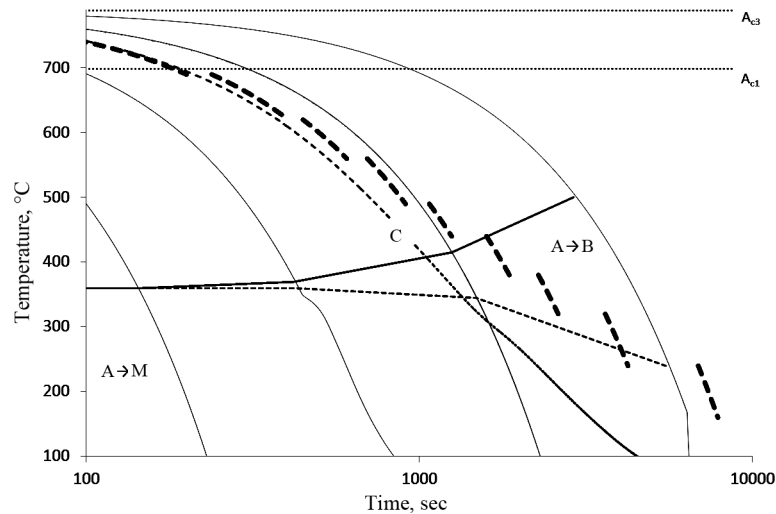
Fig. 9. Fragment of steel 18Kh2N4MA thermokinetic diagram with application of experimental trajectories for specimen cooling in a container with cast iron turnings (C) and for corresponding breakdown of experimental trajectories at constant cooling rates for temperature ranges (thick dotted).

on the TKD to the left of the constant cooling rate of 0.3°C/sec (see Fig. 2d). However, the microstructure of steel 18Kh2N4MA obtained with a constant cooling rate of 0.13°C/sec under dilatometric experiment conditions (see Fig. 3d) contains a very insignificant amount of upper bainite prepared with experimental cooling of specimens within a container with cast iron shavings (see Fig. 8c). This is connected with a variable cooling rate for specimens during heat treatment (see Fig. 1). In this case for more precise evaluation of the microstructure formed during cooling at variable rates it is necessary to use (instantaneous) cooling rates within different temperatures ranges and their relationship with the corresponding dilatometric curves as shown in Fig. 9 for steel 18Kh2N4MA. In this case it becomes understandable that the amount of bainite within the steel 18Kh2N4MA structure after cooling within a container with cast iron shavings will be significantly greater than proposed initially with direct application of cooling trajectories on TDK, which is confirmed in practice.

Steel 25Kh2N4MA, in spite of very similar chemical composition, is considerably surpassed with respect to impact strength (0.40–0.50 MJ/m^2) by steel 18Kh2N4MA (1.05–1.45 MJ/m^2) within the whole range of cooling intensity values (see Fig. 7). This is mainly connected with the higher carbon content in steel 25Kh2N4MA that provides on one hand higher strength and on the other facilitates carbide formation including during bainite formation. In addition, after slow cooling in the container the structure of steel 25Kh2N4MA contains a smaller amount of bainite than steel 18Kh2N4MA that is also is expressed to a lesser extent than a reduction in strength.

With a reduction in cooling intensity from 25°C/sec (oil quenching) to 1°C/sec (cooling in still air) the impact strength of steels 25KhN3MA and 25Kh2GSMA increases somewhat (see Fig. 7). This due to development within the structure of upper and lower bainite (Fig. 10a, b). With a further reduction in cooling intensity a marked reduction in impact strength is observed: for steel 25Kh2GSMA from 0.75 to 0.48 MJ/m^2; for steel 25KhN3MA from 0.65 to 0.42 MJ/m^2; for steel 30Kh3MF from 0.48 to 0.35 MJ/m^2. This is mainly connected with a change in bainite morphology and an increase within the structure of the proportion of coarse upper bainite with unfavorable morphology. Formation of upper bainite with slow cooling in a container is accompanied by more significant redistribution of carbon between α-phase and untransformed austenite, and also more active carbide phase precipitation than during air cooling. As a result of this alongside α-phase, bainite and coarse carbide precipitates with a further reduction in cooling there is formation of coarse high-carbon martensite from untransformed austenite rich in carbon (Fig. 10c, d). Compared with steel 18Kh2N4MA steel 25KhN3MA
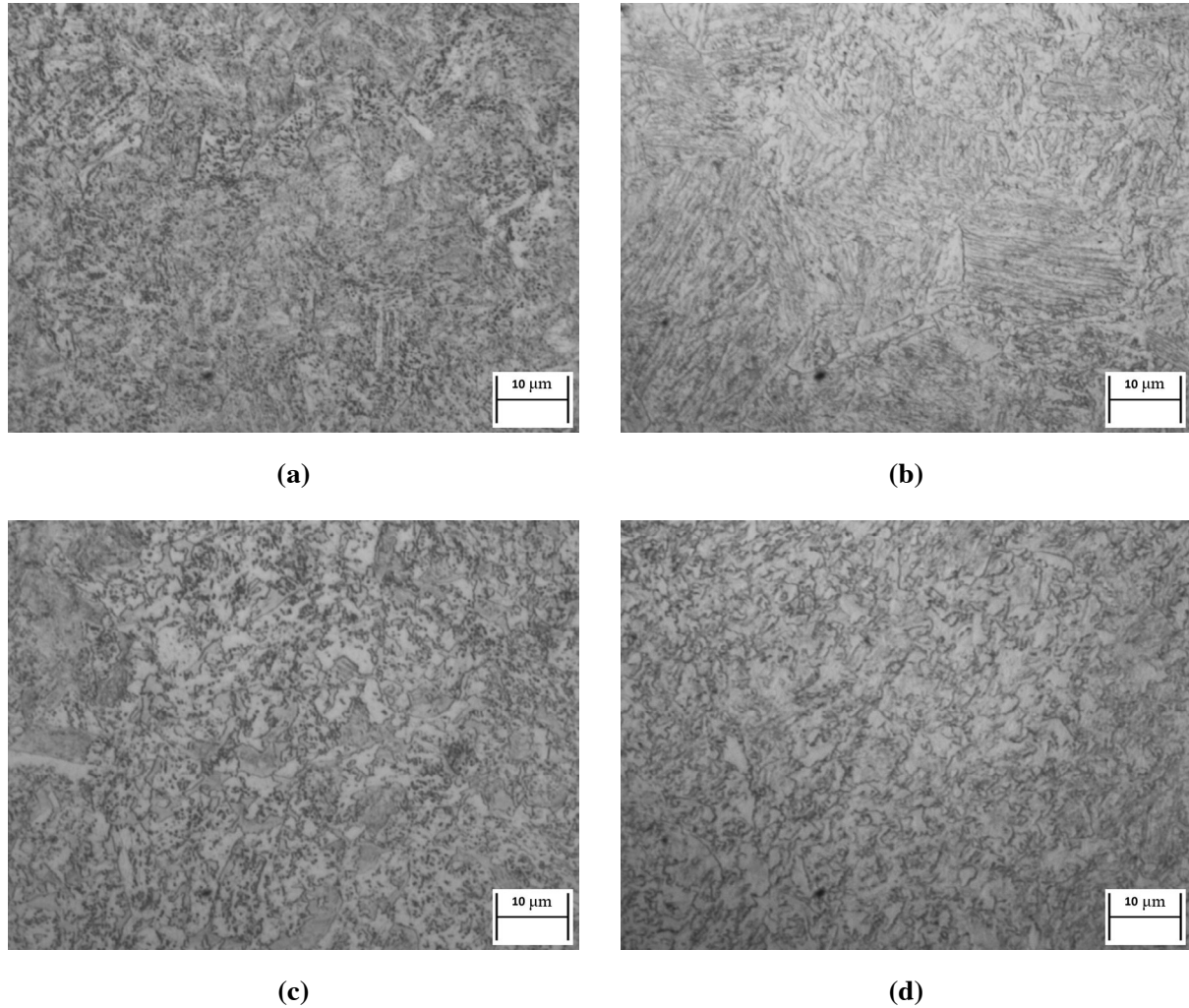
Fig. 10. Microstructure of steels 25KhN3MA (a, c) and 25Kh2GSMA (b, d)after cooling in still air (a, b is cooling rate of 1°C/sec) and within a container with cast iron turning (c, d is cooling rate of 0.2°C/sec).

contains less nickel by a factor of 1.5 and a greater amount of carbon by a factor of 1.4 as a result of which upper bainite α-phase and martensite ductility appear to be lower, and the number of embrittling carbide particles is significantly greater. This hypothesis is also valid for steel 25Kh2GSMA that hardly contains nickel, and for steel 30Kh3MFA alloyed with strong carbide-forming elements.

Comparative analysis of test steel mechanical properties showed (Fig. 11) that the on the whole the results obtained satisfy features reflecting a reduction in impact strength with an increase in strength which is caused not only by structural condition (corresponding to the ratio of bainite and martensite), but also the carbon content within steel. However, mechanical properties of steels 25KhN3MA, 25Kh2GSMA, and 30Kh3MF with a structure containing upper bainite fall out of the general feature: with a reduction in strength (1250–1300 MPa) these steels are also distinguished by high impact strength, i.e., 0.3–0.5 MJ/m^2 (in contrast to steel 18Kh2N4MA, whose upper bainite with relatively low strength 1215 MPa, has high impact strength up to 1.45 MJ/m^2). This makes it possible to propose that the unfavorable effect of upper bainite on steel impact strength develops mainly with steel carbon content of more than 0.25 wt.% and with a nickel content of less than 4 wt.%.
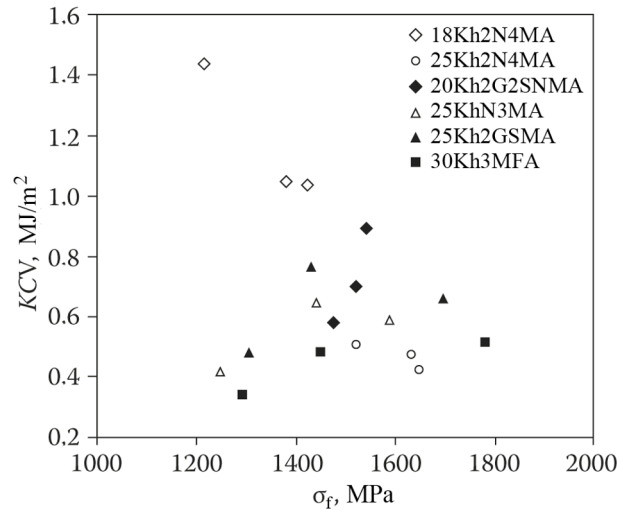
Fig. 11. Relationship of test steel strength and impact strength after cooling with different intensity.

The effect on impact strength of carbon redistribution during bainitic transformation cannot be ignored, leading to stabilization within the structure of some amount of residual austenite. As is well known [11], carbide precipitation during bainitic transformation reduces the degree of carbon redistribution between α- and γ-phases within steel. As a result of this there is a reduction in carbon concentration within untransformed residual austenite that leads to a reduction in its stability, and with action of even small impact loads there is formation of strain-induced martensite which reduces steel impact strength. In particular this explains a reduction in impact strength for steel 20Kh2G2SNMA with a reduction in cooling intensity without a marked change in morphology of the package microstructure formed, observed in an optical microscope (see Fig. 6). It should be noted that for steel 25Kh2GSMA a higher impact strength level is typical with any cooling rate than for steel 25Kh2N4MA in spite of the fact that the latter has a greater amount of nickel within the composition. This is due to an increase in the silicon content within steel 25Kh2GSMA that effectively slows down the carbide formation process also leading to stronger residual austenite stabilization.

CONCLUSIONS

The cooling rate for steels determined by experiment in various media makes it possible under laboratory conditions to evaluate the microstructure and mechanical properties that may be obtained within finished objects of steel of a specific grade during heat treatment. In this case within the bainitic and martensitic transformation temperature ranges in steels (500–200°C) the average cooling rate during oil quenching is 25°C/sec; during cooling in still air it is 1°C/sec; with cooling in a container with cast iron shavings it is 0.2°C/sec.

With variation of cooling intensity in the range 0.2–25°C/sec the least strength for all of the test steels is typical for steel 18Kh2N4MA ($\sigma_f = 1215$–1420 MPa) and the greatest stability for strength properties is distinguished for steels 20Kh2G2SNMA ($\sigma_f = 1475$–1540 MPa) and 25Kh2N4MA ($\sigma_f = 1520$–1630 MPa). In this case the impact strength of steel 20Kh2G2SNMA is 0.6–0.9 MJ/m^2), and for steel 25Kh2N4MA it is 0.4–0.5 MJ/m^2. The maximum impact strength value is observed for steel 18Kh2N4MA (1.05–1.45 MJ/m^2).

Features have been established for the change in steel impact strength with a reduction in cooling rate from 25 to 0.2°C/sec; for steels 18Kh2N4MAand 25Kh2N4MA there is a tendency towards an increase in impact

strength, more expressed with a lower carbon content; for steel 20Kh2G2SNMA there is typically a uniform reduction in impact strength; for steels 25KhN3MA, 25Kh2GSMA, and 30Kh3MF a reduction in impact strength is only observed with a reduction in cooling rate to 0.2°C/sec.

After slow cooling at a rate of 0.2°C/sec for steels 25KhN3MA, 25Kh2GSMA, and 30Kh3MF there is typically a reduction in strength $(\sigma_f = 1245–1305\ \text{MPa})$ and impact strength 0.3-0.5 MJ/m^2) which is connected with formation of upper bainite. Therefore, during development of heat treatment technology for components of these steels it is necessary to tend towards achievement of a cooling rate not less than 1°C/sec in the bainitic and martensitic transformation temperature ranges (500–200°C).

An optimum concentration of high-strength (1400 MPa or more) and impact strength (0.6 MJ/m^2 or more) differs for steels 18Kh2N4MA, 25Kh2GSMA, and 25KhN3MA after cooling at a rate of not less than 1°C/sec, and also steel 20Kh2G2SNMA after cooling in the rate range 0.2–25°C/sec. In view of this test steel 20Kh2G2SNMA as a result of forming predominantly austenite low-temperature transformation products over a wide cooling rate range provides the most stable set of properties independent of cooling rate intensity and consequently on the cross section of components subjected to heat treatment.

REFERENCES

1. S. Šolić, B. Podgornik, and V. Leskovšek, "The occurrence of quenching cracks in high-carbon tool steel depending on the austenitizing temperature," *Eng. Failure Analysis,* **92**, 140–148 (2018); DOI: 10.1016/j.engfailanal.2018.05.008.

2. N. I. Kobasko, "The development of quench cracks in steel," *Metal Science and Heat Treatment,* **12**, No. 11, 900–901 (1970); DOI: 10.1007/BF00653381.

3. E. H. Hwang, J. S. Park, S. O. Kim, H. G. Seong, and S. J. Kim, "Study on the controlling factors for the quenching crack sensitivity of ultra-strong automotive steel," *J. Mater. Sci.,* **55**. 3605–3617 (2020); DOI: 10.1007/s10853-019-04177-1.

4. M. V. Maisuradze, Yu. V. Yudin, and D. I. Lebedev, "Thermal strengthening of large parts made from high-strength sparingly doped steel in air," *Steel in Translation,* **50**, No. 5, 61–66 (2020); DOI: 10.3103/S0967091220050083.

5. M. V. Maisuradze, M. A. Ryzhkov, and D. I. Lebedev, "Microstructure and mechanical properties of martensitic high strength engineering steel," *Metallurgist,* **64**, No. 7–8, 640–651 (2020); DOI: 10.1007/s11015-020-01040-6.

6. L. M. Kleiner, A. A. Shatsov, and D. M. Larinin, "Low-carbon martensitic steels. Alloying and properties," *Metal Science and Heat Treatment,* **52**, No. 11–12, 540–544 (2011); DOI: 10.1007/s11041-011-9316-z.

7. Yu. N. Simonov, O. D. Panov, M. Yu. Simonov, V. P. Vylezhnev, and A. S. Ivanov, "Principles of design of the chemical composition of steels for forming a structure of lower carbide-free bainite under delayed cooling," *Metal Science and Heat Treatment,* **57**, No. 7–8, 386–394 (2015); DOI: 10.1007/s11041-015-9894-2.

8. A. N. Yurchenko, Yu. N. Simonov, D. O. Panov, and A. I. Zhitenev, "Transformations, structure and properties of steel 22Kh2G2S2MF under continuous cooling," *Metal Science and Heat Treatment,* **61**, No. 9–10, 617–621 (2019); DOI: 10.1007/s11041-02000469-5.

9. J. Yin, M. Hillert, and A. Borgenstam, "Morphology of upper and lower bainite with 0.7 mass pct. C," *Metallurgical and Materials Transactions A,* **48**, 4006–4024 (2017); DOI: 10.1007/s11661-017-4208-5.

10. O. Hajizad, A. Kumar, Z. Li, R .H. Petrov, J. Sietsma, and R. Dollevoet, "Influence of microstructure on mechanical properties of bainitic steels in railway applications," *Metals,* **9**, No. 7, 778 (2019); DOI: 10.3390/met9070778.

11. H. K. D. H. Bhadeshia, *Bainite in Steels. Theory and Practice,* Maney Publishing, Leeds, UK (2015)

12. M. V. Maisuradze and M. A. Ryzhkov, "Microstructure and mechanical properties of the heat treated HY-TUF steel," *Materials Science Forum,* **989**, 324–328 (2020); DOI:10.4028/ www.scientific.net/MSF.989.324.

13. M. V. Maisuradze, Yu. V. Yudin, and A. A. Kuklina, "Increase in impact strength during bainite structure formation in HYTUF high-strength steel," *Metallurgist,* **63**, No. 7–8, 849–858 (2019); DOI: 10.1007/s11015-019-00899-4.

14. M. V. Maisuradze, M. A. Ryzhkov, E. V. Antakov, N. A. Popov, and P. A. Proskuryakov, "Special features of transformations of supercooled austenite in modern structural steels," *Metal Science and Heat Treatment,* **62**, No. 7–8, 448– 456 (2020); DOI: 10.1007/s11041-020-00583-4.

15. H. K. D. H. Bhadeshia and R. Honeycombe, *Steels: Microstructure and Properties*, Butterworth-Heinemann, UK (2017).

16. L. E. Popova and A. A. Popov, *Transformation Diagram for Austenite in Steels and* β *-Solution in Titanium Alloys. Reference* [in Russian], Metallurgiya, Moscow (1991).

17. M. V. Maisuradze, M. A. Ryzhkov, and Yu. V. Yudin, "Rapid evaluation of the cooling capacity of quenching media," *Metal Science and Heat Treatment*, **57**, No. 7–8, 515–518 (2015); DOI: 10.1007/s11041-015-9914-2.

18. ASTM D6200-01. *Standard Test Method for Determination of Cooling Characteristics of Quench Oils by Cooling Curve Analysis*, West Conshohocken: ASTM International (2017).

19. G. E., Totten, G. M. Webster, H. M. Tens, and B. Liscic, "Standards for cooling curve analysis of quenchants," *Heat Treatment of Metals*, No. 4, 92–94 (1997).

20. P. C. Angelo and B. Ravisankar, *Introduction to Steels. Processing, Properties, and Applications*, CRC Press, Boca Raton (2019).